Chapter 5
Strain Fields and Electronic Structure of Vacancy-Type Defects in Graphene from First-Principles Simulation

A.V. Krasheninnikov

Abstract Using density-functional-theory simulations we study strain fields near vacancy-type defects in graphene. We demonstrate that the strain fields around these defects reach far into the unperturbed hexagonal network. As metal and other adatoms have a high affinity to the non-perfect and strained regions of graphene, they are therefore attracted by the reconstructed defects. This explains the intriguing behavior of metal adatoms on graphene reported in recent experiments (Cretu et al., Phys Rev Lett 105:196102, 2010). Finally, we analyze the electronic band structure of graphene with defects and show that some defects open a semiconductor gap in graphene, which may be important for carbon-based nanoelectronics.

Keywords Graphene • Defects • Electronic structure calculations

5.1 Introduction

Recent reports on the electronic and mechanical properties of graphene [1], a novel two-dimensional (2D) material made from carbon with a honeycomb-like arrangement of atoms, indicate that graphene is a promising candidate for the next generation electronics. The electronic and mechanical properties of graphene samples with high perfection of the atomic lattice are exceptional [2]. For example, semimetallic graphene has alinear dispersion relation and high mobility of charge carriers [3], while its Young's modulus is about 1 TPa [4], the highest among all known.

A.V. Krasheninnikov (✉)
Department of Applied Physics, Aalto University, P.O. Box 1100, Helsinki FI-0076, Finland

Department of Physics, University of Helsinki, P.O. Box 43, Helsinki FI-00014, Finland
e-mail: Arkady.Krasheninnikov@helsinki.fi

Y.N. Shunin and A.E. Kiv (eds.), *Nanodevices and Nanomaterials for Ecological Security*, NATO Science for Peace and Security Series B: Physics and Biophysics, DOI 10.1007/978-94-007-4119-5_5,

One should bear in mind, however, that structural defects [5] that may appear during the growth or processing, should deteriorate graphene properties and the performance of graphene-based devices. At the same time, deviations from the perfection can also be useful in some applications, as they make it possible to tailor the local properties of graphene and to achieve new functionalities, for example, by opening a semiconducting gap [6, 7] required for the operation of graphene-based transistors.

Foreign atoms can also be incorporated into graphene as substitutional impurities forming extrinsic defects. In this case, the impurity atom replaces one or two carbon atoms. Boron or nitrogen serve as the natural dopants in carbon nanostructures [8–13] since they have one electron less or more, respectively, but roughly the same atomic radius. This mechanism of graphene doping has received a particular attention, alongside with mechanisms [14, 15] based on the adsorption of organic molecules as well as metal atoms and clusters.

Much larger atoms such as transition metal (TM) impurities [16–18] can be incorporated into the atomic network as well, or added as adatoms. This issue has received lots of attention in the context of the unconventional Kondo effect in graphene and spintronics [19–22], its doping [3] and possible catalysis [23]. Furthermore, the precise knowledge of the details of TM–sp^2-carbon interaction is important for understanding the carbon nanotube growth [24], fuel cell properties [25], and the role of implanted magnetic atoms such as Fe in the development of magnetic order in carbon materials [26].

Previous experimental [17, 27] and theoretical studies [16–18, 28, 29] have demonstrated that the preferred way to incorporate TM impurities in graphene is to attach them to vacancies. Substitutional dopants are expected to be very stable due to the strong covalent bonding of TM atoms to the host carbon matrix. The binding energies for the TM-vacancy complexes have been reported to be in the range of 2–8 eV [16, 28, 29], indicating strong bonding, and pointing to a possible use of such structures in catalysis. It has also been suggested [16] to use spatially-localized electron irradiation to create defects with atomic precision and then, by making co-deposited metal atoms, mobile them at elevated temperatures, to pin the atoms at the defects. This idea has been experimentally implemented [30] for Fe, Co, and Mo atoms.

However, substitutional impurities are strong scatterers of electronic states in graphene [3], and alternative ways for implementing spatially-localized doping has been searched for. Recent experiments [17] on W atoms on defected graphite have indicated that the bonding may be more complicated than the simple model of substitutional impurities predicts. The strong bonding (e.g., 8.6 or 8.9 eV for a tungsten atom trapped in a single or double vacancy, respectively) is inconsistent with the thermal and possibly irradiation-induced migration observed in the experiments. To explain the contradiction, it has been suggested [17] that reconstructed point defects in graphene created by electron irradiation and annealing can also pin the adatoms. It has been shown that the strain field around a reconstructed divacancy (the so-called 555-777 defects) reaches far into the unperturbed hexagonal network and that metal atoms have a high affinity to the non-perfect and strained regions of graphene. Metal atoms are therefore attracted by reconstructed defects and bonded with energies of the order of 2 eV.

In the present paper, we focus on the strain fields near all reconstructed vacancy-type defects. By employing first-principles simulation, we visualize the strain fields near vacancy-type defects in graphene and demonstrate that such defects create areas with the size of 2–3 nm where adatoms are attracted to the defects. We further calculate the electronic structure of the most important vacancy-type defects.

5.2 Computational Details

The density functional theory (DFT) *ab initio* calculations have been carried out with the VASP simulation package [31] using projector augmented wave (PAW) potentials [32] to describe core electrons, and the Generalized Gradient Approximation of Perdew, Burke and Ernzernhof (PBE) [33] for exchange and correlation. The kinetic energy cutoff for the plane waves was set to 400 eV, and all structures were relaxed until atomic forces were below 0.01 eV/ÅA. Increasing the cutoff energy up to 600 eV changed the bonding energies by less than 10 meV. The sampling scheme of Monkhorts-Pack [34] with up to $9 \times 9 \times 1$ k-points meshes was used to integrate over the Brillouin zone.

Graphene was modeled as a supercell composed from 10×10 graphene unit cells so that the initial structure, in which the defects were introduced, consisted of 200 carbon atoms. The unit cell is shown in Fig. 5.1.

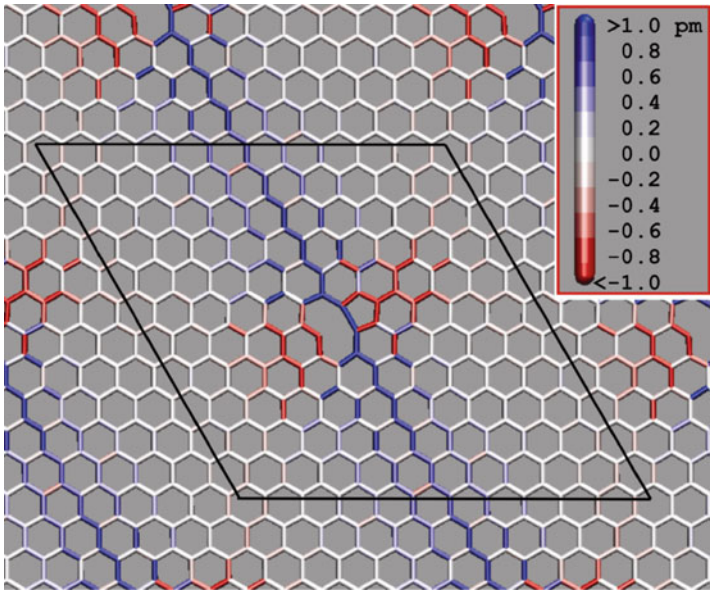

Fig. 5.1 Atomic structures of a single vacancy in a graphene sheet. The bonds are colored according to an increase (*blue*) or decrease (*red*) in the bond length (given in picometers). The bonds close to pentagons are contracted, but most C–C bonds are stretched. The *black lines* outline the simulation supercell (10×10) graphene units

5.3 Results

5.3.1 Strain Fields Near Vacancy-Type Defects

The most prolific defects produced by energetic electrons in graphene are vacancies [35]. Single vacancies (SV) in graphene [36, 37] and nanotubes [38, 39] undergo a Jahn-Teller distortion, which leads to the saturation of two of the three dangling bonds towards the missing atom. One dangling bond always remains due to the geometrical reasons, Fig. 5.1. It is intuitively clear that due to the presence of an under-coordinated carbon atom, and a lower displacement threshold for this atom [40], SV should be quickly transformed to a di-vacancy (DV), which can also be referred to as a 5-8-5 defect. The DV also reconstructs, so that two new weak bonds are formed, lowering the energy of the system.

Besides, at elevated temperatures (over 200°C), SVs also transform to DVs due to SV migration and coalescence [41]. DVs undergo further transformations to 555-777 [42] and 5555-6-7777 defects by bond rotations, as this process lowers the total energy of the system by more than 1 eV per defect. The atomic structures of these defects are presented in Fig. 5.2. Note that in panels (a–d) the same number of carbon atoms (two) are missing.

Previous simulations [17] have shown that the binding (adsorption) energy (negatively defined) near a 555-777-defect decreases and that the drop in energy can be explained by a combination of two effects: strain fields near the defects and the decrease in the adsorption energy of the adatom on top of strained bonds. All these give rise to the effective attraction of the adatoms by the defects.

In order to better understand the mechanism of the attractive interaction, we calculated strain fields near the SV, Fig. 5.1 as well as DV and related defects, Fig. 5.2. The strain fields were visualized as the difference between the bond lengths in the system with a defect and that in the pristine sheet. It is evident that all vacancy-type defects give rise to strain fields in their vicinity, with the range of at least 2–3 nm or possibly even more (larger than the supercell). Most C–C bonds are stretched, but the bonds close to pentagons are contracted, as graphene is an elastic material with a finite value of Poisson ratio [43].

5.3.2 Strain Fields Near Adatoms on Pristine Graphene

As W adatoms on graphene have been used in recent experiments [17], we calculated the strain fields near W adatoms on pristine graphene. The existence of a strain field of opposite sign (with regard to vacancy-type defect) could have explained the attractive interaction between vacancies and adatoms. However, in a two-dimensional system the weakly bonded W adatom does not create a long-range strain field of the opposite sign in the carbon network, Fig. 5.3b, c, and the

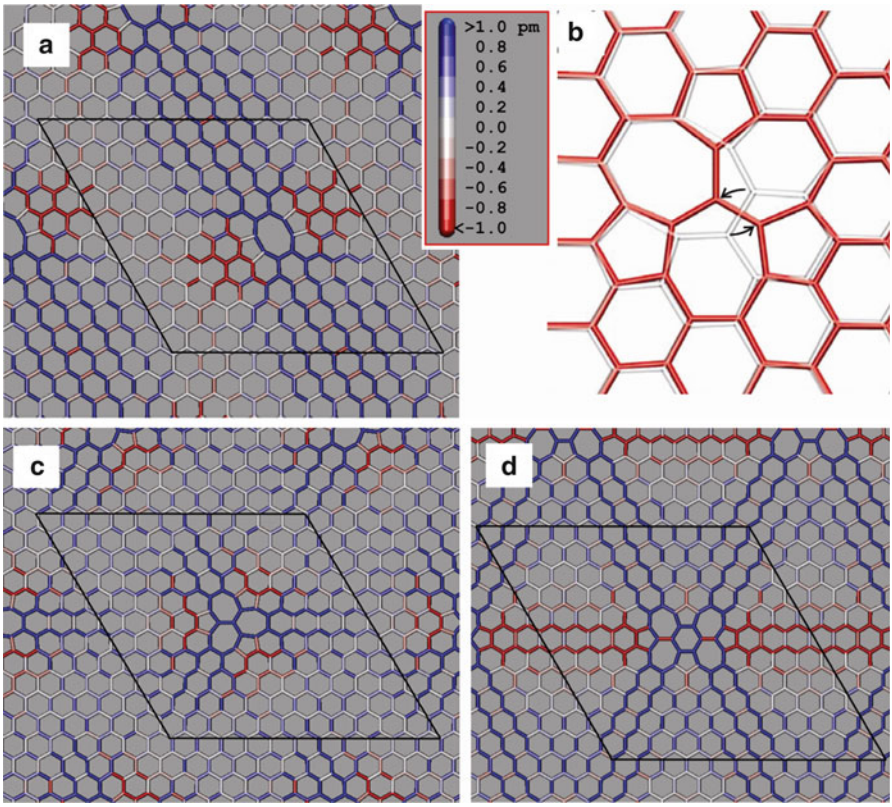

Fig. 5.2 Atomic structures of a di-vacancy 5-8-5 defect (**a**), and the reconstructed di-vacancy defect including the 555-777 (**c**) and 5555-6-7777 defect (**d**). The latter defects were obtained by rotating one of the carbon bonds in the di-vacancy defect, as schematically shown in panel (**b**). Such defects have lower energies as the parent structure shown in panel (**a**). The bonds are colored according to an increase (*blue*) or decrease (*red*) in the bond length (given in picometers). The bonds close to pentagons are contracted, but most C–C bonds are stretched. The *red lines* outline the simulation supercell (10 × 10 graphene units). It is evident that the strain fields extend for at least 2 nm away from the defect

conventional mechanism of vacancy-interstitial attraction as in 3D bulk systems it does not work.

We have not found any long-range strain fields near other adatoms, we have studied (W, Cr, Mo). This is an expected result, as adatom binding energy to graphene sheet is relatively small, about 0.5 eV, and the adatom is well outside the plane.

We have also calculated the strain fields near carbon adatoms. Interestingly enough, even carbon adatoms which bind relatively strongly to graphene [44] and nanotubes [45] with energies 1–3 eV also give rise to changes in the bond lengths between the nearest neighbors of the adatom only, so that no long-range strain effect is present. Thus, vacancy and interstitial-type defects (adatoms) in graphene do not interact via strain fields of opposite sign, as in the majority of bulk materials.

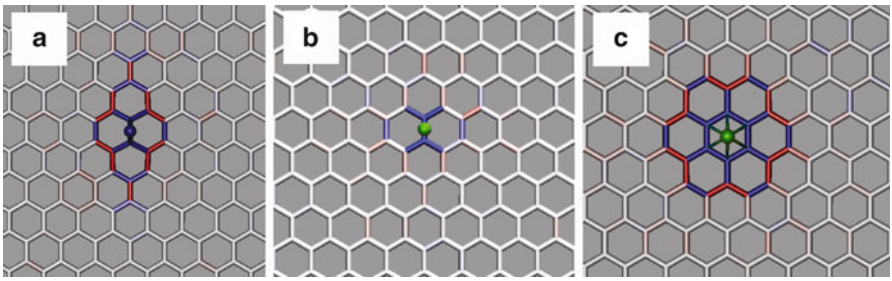

Fig. 5.3 Atomic structure of the graphene sheet with adatoms and strain fields near the adatom. (**a**) Carbon adatom. (**b**) W adatom in the bridge and middle-of-hexagon (**c**) positions. The bonds are colored according to the increase (*blue*) or decrease (*red*) in the bond length (given in picometers) with regard to the pristine system. It is evident that there is no considerable long-ranged strain field. The coloring scheme is the same as in the case of the vacancy-type defects shown in Fig. 5.2. The *balls* represent the adatoms

We calculated earlier [17] the adsorption energy of the W adatom on the strained graphene sheet. The results prove that a biaxial strain of 1% (resp. 2%) lowers the energy for the middle-of-hexagon position from initially −0.38 to −0.54 (−0.69) eV, and for the bridge position from −0.45 to −0.52 (−0.59) eV, respectively.

The drop in energy and stronger bonding can be associated with a smaller saturation of the C–C bonds under strain, so that more electron density is available for making a new bond with the adatom. The observed energy gradient comes from a combination of the strain field and electronic effects. This observation points out towards possible applications of graphene ribbons as strain sensors, as a drop in adsorption energy should increase the number of adsorbed species and thus affect the current through graphene ribbon [46]. The attractive interaction between the adatoms and defects is different from the known phenomenon of long-range interactions of adatoms on metals [47], graphite [48], or carbon nanotubes [49], which is mediated by purely electronic effects [50].

5.3.3 *Electronic Structure of Vacancy-Type Defects*

As the effects of point defects and impurities on the electronic structure of graphene presents considerable interest in the context of defect-mediated engineering of graphene electronic properties, we have also calculated the band structure of graphene with the most stable vacancy-type defects, 555-777 and 5555-6-7777 configurations. For the sake of comparison, we also present here the band structures of SV and DV, although these defects are less stable than the 555-777 and 5555-6-7777 defects.

The band structure of a 200 atom supercell with a 555-777-defect is shown in Fig. 5.4a.

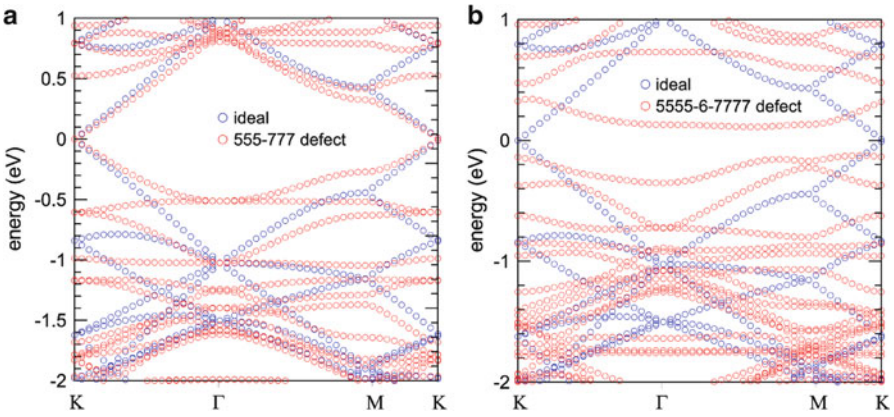

Fig. 5.4 Band structure of graphene 200-atom supercell with a 555-777 defect (**a**) and 5555-6-7777 defect (**b**). Note that for the 5555-6-7777 defect a gap about 0.3 is open. Zero energy corresponds to the position of the Fermi level in pristine graphene

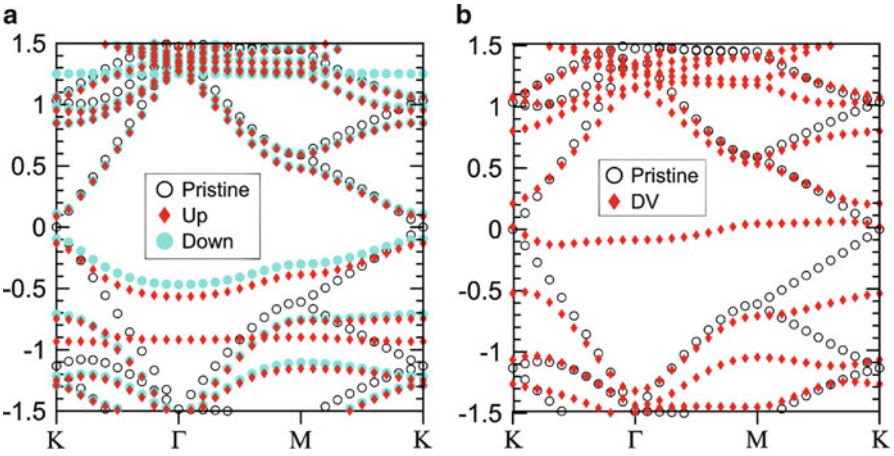

Fig. 5.5 Band structure of graphene 98-atom supercell with a single vacancy (**a**) and double vacancy defect (**b**)

It is evident that, although the defect gives rise to new localized states below the Fermi level (0.5 eV), it does not alter the electronic structure of graphene sheet at the Fermi level. Thus, one can expect that a TM atom-555-777 complex will be a weaker scattering center than the substitutional impurity, and thus the preferable way to incorporate TM atoms into the system.

The situation is quite different in the case of the 5555-6-7777-defect. A gap of more than 0.3 eV is opened at the Fermi level. The gap is much larger than that for SV and DV, about 0.1 eV, Fig. 5.5, which agrees with the previously published results [51].

Besides, as it has been mentioned above, the non-reconstructed SV and DV are less stable than the reconstructed defects, so that their probability to exist is smaller. Our results [7] indicate that a gap is always opened near complicated vacancy-type defects in graphene, when rotated hexagons, Fig. 5.2d are embedded into graphene through non-hexagonal rings (pentagons and heptagons). This result may be important for nanoelectronics, and spatially localized electron or ion irradiation [35, 52–56] can be used to produce such areas.

5.4 Conclusions

We have studied at length the stain filed near vacancy-type defects in graphene. We have shown that the 555-777-type reconstructed vacancies, which are the predominant defects in a wide temperature range, create long-ranged strain fields in their vicinity and thus are efficient trapping centers for metal adatoms. Metal atoms migrating on graphene are attracted by these defects at distances in the nanometer range. The interaction between defects in graphene and metal atoms is different from the known mechanisms of strain fields and electronic effects in bulk systems and on their surfaces, and originates from an interplay of local strain in the atomic network, created by the defect, and electronic adsorption effects.

The trapping of metal atoms in strained areas and at defects in graphene may be used for engineering the local electronic and magnetic structure of graphene and its doping by the controlled production of defects. Finally, we have analyzed the band structure of graphene with defects and have shown that some defects open a semiconductor gap in graphene, which may be important for the development of carbon-based nanoelectronics.

Acknowledgements We thank F. Banhart for useful discussions. This work has been supported by the Academy of Finland through Centers of Excellence and other projects. The Finnish IT Center for Science has provided generous grants of computer time.

References

1. Novoselov KS, Geim AK, Morozov SV, Jiang D, Katsnelson MI, Grigorieva IV, Dubonos SV, Firsov AA (2005) Two-dimensional gas of massless Dirac fermions in graphene. Nature 438:197
2. Geim AK, Novoselov KS (2007) The rise of graphene. Nat Mater 6:183
3. Castro Neto AH, Guinea F, Peres NMR, Novoselov KS, Geim AK (2009) The electronic properties of graphene. Rev Mod Phys 81:109
4. Lee C, Wei X, Kysar JW, Hone J (2008) Measurement of the elastic properties and intrinsic strength of monolayer graphene. Science 321:385
5. Banhart F, Kotakoski J, Krasheninnikov AV (2011) Structural defects in graphene. ACS Nano 5:26

6. Appelhans DJ, Lin Z, Lusk MT (2010) Two-dimensional carbon semiconductor: density functional theory calculations. Phys Rev B 82:073410
7. Kotakoski J, Krasheninnikov AV, Kaiser U, Meyer JC (2011) From point defects in graphene to two-dimensional amorphous carbon. Phys Rev Lett 106:105505
8. Wang X, Li X, Zhang L, Yoon Y, Weber PK, Wang H, Guo J, Dai H (2009) N-Doping of graphene through electrothermal reactions with ammonia. Science 324:768
9. Reddy ALM, Srivastava A, Gowda SR, Gullapalli H, Dubey M, Ajayan PM (2010) Synthesis of nitrogen-doped graphene films for lithium battery application. ACS Nano 4:6337
10. Biel B, Blase X, Triozon F, Roche S (2009) Anomalous doping effects on charge transport in graphene nanoribbons. Phys Rev Lett 102:096803
11. Zheng XH, Rungger I, Zeng Z, Sanvito S (2009) Effects induced by single and multiple dopants on the transport properties in zigzag-edged graphene nanoribbons. Phys Rev B 80:235426
12. Dutta S, Manna AK, Pati SK (2009) Intrinsic half-metallicity in modified graphene nanoribbons. Phys Rev Lett 102:096601
13. Krivanek OL, Chisholm MF, Nicolosi V, Pennycook TJ, Corbin GJ, Dellby N, Murfitt MF, Own CS, Szilagyi ZS, Oxley MP, Pantelides ST, Pennycook SJ (2010) Atom-by-atom structural and chemical analysis by annular dark-field electron microscopy. Nature 464:571
14. Pinto H, Jones R, Goss J, Briddon PR (2010) Mechanisms of doping graphene. Phys Status Solidi (a) 207:2131
15. Subrahmanyam K, Manna AK, Pati SK, Rao CNR (2010) A study of graphene decorated with metal nanoparticles. Chem Phys Lett 497:70
16. Krasheninnikov AV, Lehtinen PO, Foster AS, Pyykkö P, Nieminen RM (2009) Embedding transition-metal atoms in graphene: structure, bonding, and magnetism. Phys Rev Lett 102:126807
17. Cretu O, Krasheninnikov AV, Rodriguez-Manzo JA, Sun L, Nieminen R, Banhart F (2010) Migration and localization of metal atoms on strained graphene. Phys Rev Lett 105:196102
18. Zhang W, Sun L, Xu Z, Krasheninnikov AV, Huai P, Zhu Z, Banhart F (2010) Migration of gold atoms in graphene ribbons: role of the edges. Phys Rev B 81:125425
19. Hentschel M, Guinea F (2007) Orthogonality catastrophe and Kondo effect in graphene. Phys Rev B 76:115407
20. Sengupta K, Baskaran G (2008) Tuning Kondo physics in graphene with gate voltage. Phys Rev B 77:045417
21. Dóra B, Thalmeier P (2007) Reentrant Kondo effect in Landau-quantized graphene: influence of the chemical potential. Phys Rev B 76:115435
22. Shytov AV, Katsnelson MI, Levitov LS (2007) Vacuum polarization and screening of supercritical impurities in graphene. Phys Rev Lett 99:236801
23. Bittencourt C, Felten A, Douhard B, Colomer J-F, Van Tendeloo G, Drube W, Ghijsen J, Pireaux J-J (2007) Metallic nanoparticles on plasma treated carbon nanotubes: nanohybrids. Surf Sci 601:2800
24. Yazyev OV, Pasquarello A (2008) Effect of metal elements in catalytic growth of carbon nanotubes. Phys Rev Lett 100:156102
25. Che G, Lakshmi BB, Fisher ER, Martin CR (1998) Carbon nanotubule membranes for electrochemical energy storage and production. Nature 393:346
26. Sielemann R, Kobayashi Y, Yoshida Y, Gunnlaugsson HP, Weyer G (2008) Magnetism at single isolated Iron atoms implanted in graphite. Phys Rev Lett 101:137206
27. Gan Y, Sun L, Banhart F (2008) One- and two-dimensional diffusion of metal atoms in graphene. Small 4:587
28. Santos EJG, Ayuela A, Fagan SB, Mendes Filho J, Azevedo DL, Souza Filho AG, Sánchez-Portal D (2008) Switching on magnetism in Ni-doped graphene: density functional calculations. Phys Rev B 78:195420
29. Santos EJG, Ayuela A, Sánchez-Portal D (2010) First-principles study of substitutional metal impurities in graphene: structural, electronic and magnetic properties. New J Phys 12:053012

30. Rodriguez-Manzo JA, Cretu O, Banhart F (2010) Trapping of metal atoms in vacancies of carbon nanotubes and graphene. ACS Nano 4:3422
31. Kresse G, Furthmüller J (1996) Efficiency of ab–initio total energy calculations for metals and semiconductors using a plane–wave basis set. Comput Mater Sci 6:15
32. Blöchl PE (1994) Projector augmented-wave method. Phys Rev B 50:17953
33. Perdew JP, Burke K, Ernzerhof M (1996) Generalized gradient approximation made simple. Phys Rev Lett 77:3865
34. Monkhorst HJ, Pack JD (1976) Special points for Brillouin-zone integrations. Phys Rev B 13:5188
35. Krasheninnikov AV, Banhart F (2007) Engineering of nanostructured carbon materials with electron or ion beams. Nat Mater 6:723
36. Lehtinen PO, Foster AS, Ma Y, Krasheninnikov AV, Nieminen RM (2004) Irradiation-induced magnetism in graphite: a density functional study. Phys Rev Lett 93:187202
37. El-Barbary AA, Telling RH, Ewels CP, Heggie MI, Briddon PR (2003) Structure and energetics of the vacancy in graphite. Phys Rev B 68:144107
38. Krasheninnikov AV, Nordlund K, Sirviö M, Salonen E, Keinonen J (2001) Formation of ion irradiation-induced atomic-scale defects on walls of carbon nanotubes. Phys Rev B 63:245405
39. Krasheninnikov AV (2001) Predicted scanning microscopy images of carbon nanotubes with atomic vacancies. Solid State Commun 118:361
40. Krasheninnikov AV, Banhart F, Li JX, Foster AS, Nieminen R (2005) Stability of carbon nanotubes under electron irradiation: role of tube diameter and chirality. Phys Rev B 72:125428
41. Krasheninnikov AV, Lehtinen PO, Foster AS, Nieminen RM (2006) Bending the rules: contrasting vacancy energetics and migration in graphite and carbon nanotubes. Chem Phys Lett 418:132
42. Lee G, Wang CZ, Yoon E, Hwang N, Kim D, Ho KM (2005) Diffusion, coalescence, and reconstruction of vacancy defects in graphene layers. Phys Rev Lett 95:205501
43. Scarpa F, Adhikari S, Phani AS (2010) Effective elastic mechanical properties of single layer graphene sheets. Nanotechnology 20:065709
44. Lehtinen PO, Foster AS, Ayuela A, Krasheninnikov A, Nordlund K, Nieminen RM (2003) Magnetic properties and diffusion of adatoms on a graphene sheet. Phys Rev Lett 91:017202
45. Krasheninnikov AV, Nordlund K, Lehtinen PO, Foster AS, Ayuela A, Nieminen RM (2004) Adsorption and migration of carbon adatoms on zigzag nanotubes. Carbon 42:1021
46. Schedin F, Geim AK, Morozov SV, Hill EW, Blake P, Katsnelson MI, Novoselov KS (2007) Detection of individual gas molecules adsorbed on graphene. Nat Mater 6:652
47. Repp J, Moresco F, Meyer G, Rieder K-H (2000) Substrate mediated long-range oscillatory interaction between adatoms: Cu/Cu(111). Phys Rev Lett 85:2981
48. Hornekær L, Rauls E, Xu W, Šljivančanin Ž, Otero R, Stensgaard I, Lægsgaard E, Hammer B, Besenbacher F (2006) Clustering of chemisorbed H(D) atoms on the graphite (0001) surface due to preferential sticking. Phys Rev Lett 97:186102
49. Buchs G, Krasheninnikov AV, Ruffieux P, Gööning P, Foster AS, Nieminen RM, Gröning O (2007) Creation of paired electron states in the gap of semiconducting carbon nanotubes by correlated hydrogen adsorption. New J Phys 9:275
50. Cheianov VV, Fal'ko VI (2006) Friedel oscillations, impurity scattering, and temperature dependence of resistivity in graphene. Phys Rev Lett 97:226801
51. Santos EJG, Sánchez-Portal D, Ayuela A (2010) Magnetism of substitutional co impurities in graphene: realization of single π vacancies. Phys Rev B 81:125433
52. Krasheninnikov AV, Miyamoto Y, Tománek D (2007) Role of electronic excitations in ion collisions with carbon nanostructures. Phys Rev Lett 99:016104
53. Compagnini G, Giannazzo F, Sonde S, Raineri V, Rimini E (2009) Ion irradiation and defect formation in single layer graphene. Carbon 47:3201

54. Åström JA, Krasheninnikov AV, Nordlund K (2004) Carbon nanotube mats and fibers with irradiation-improved mechanical characteristics: a theoretical model. Phys Rev Lett 93:215503; (2005) 94:029902(E)
55. Lemme MC, Bell DC, Williams JR, Stern LA, Baugher BWH, Jarillo-Herrero P, Marcus CM (2009) Etching of graphene devices with a helium ion beam. ACS Nano 3:2674
56. Krasheninnikov AV, Nordlund K (2010) Ion and electron irradiation-induced effects in nanostructured materials. J Appl Phys 107:071301